Syntheses and Crystal Structures of Ruthenium-Salen Complexes Containing Triphenylphosphine Ligands

Yan Li[a,b], Qing Ma[a,b], Hua-Tian Shi[b], Qun Chen[a], and Qian-Feng Zhang[a,b]

[a] School of Chemistry and Chemical Engineering, Changzhou University, Jiangsu 213164, P. R. China
[b] Institute of Molecular Engineering and Applied Chemistry, Anhui University of Technology, Ma'anshan, Anhui 243002, P. R. China

Reprint requests to Dr. Qian-Feng Zhang.
Fax: +86-555-2312041.
E-mail: zhangqf@ahut.edu.cn

Z. Naturforsch. **2011**, *66b,* 324 – 328;
received October 27, 2010

Treatment of $[Ru(PPh_3)_3Cl_2]$ with the Schiff base ligand H_2salen in THF at reflux afforded a neutral Ru^{III}-salen complex $[Ru^{III}(salen)(PPh_3)Cl]$ (**1**). Interaction of $[RuHCl(CO)(PPh_3)_3]$ with H_2salen under similar conditions gave a neutral Ru^{II}-salen complex $[Ru^{II}(salen\text{-}NH)(PPh_3)(CO)]$ (**2**). In its formation one of the imine bonds was nucleophilically attacked by hydride to give a mixed imine-amine ligand. The two complexes have been spectroscopically characterized, and the crystal structures of $\mathbf{1} \cdot 2CH_2Cl_2$ and $\mathbf{2} \cdot CH_2Cl_2$ have been established by X-ray crystallography.

Key words: Ruthenium, Schiff Base Ligand, Salen, Synthesis, Crystal Structure

Introduction

Ruthenium complexes are currently investigated because of their interesting structural, electrochemical, catalytic, and biological properties [1–5] including research of ruthenium complexes containing diimino tetradentate Schiff bases, such as salen and salophen ligands [6, 7]. It has been noted that manganese-salen complexes can be widely used as catalysts for alkene epoxidation [8]. Recently, a number of ruthenium-salen complexes have also been found to be active catalysts in various chemical transformations [9, 10]. In particular, ruthenium macrocyclic complexes which are stable towards demetalation have been found to show a reversible electrochemistry and provide good model systems for mechanistic investigations of proton-coupled multielectron transfer reactions [11, 12]. To design rationally transformations catalyzed by ruthenium-salen complexes, the knowledge of their redox and structural properties is desirable [13]. A few ruthenium-salen complexes containing carbene, nitride, nitrosyl, oxo, hydrate, carbonyl, and halide groups, which show catalytic activity and wherein the ruthenium oxidation states vary from +2 to +6, have been investigated in recent years [14–18]. However, ruthenium-salen complexes with triphenylphosphine ligands have been less explored [18, 19]. We were therefore interested in the reactions of salen derivatives with the typical ruthenium(II) center starting from $[Ru(PPh_3)_3Cl_2]$ and $[RuHCl(CO)(PPh_3)_3]$, which resulted in the isolation of ruthenium(III) and ruthenium(II)-salen complexes stabilized by triphenylphosphine ligands. The initial results including the structural characterization and electrochemical properties of such ruthenium-salen complexes are presented in this paper.

Experimental Section

General

All synthetic manipulations were carried out under dry nitrogen by standard Schlenk techniques. $[Ru(PPh_3)_3Cl_2]$ [20] and $[RuHCl(CO)(PPh_3)_3]$ [21] were prepared according to the literature methods. The Schiff base ligand H_2salen (salen = *NN′*-bis(salicylidene)-*o*-phenylenediamine dianion) was synthesized by condensation of salicylaldehyde with *o*-phenylenediamine in refluxing ethanol [22]. $RuCl_3 \cdot 3H_2O$ was used as purchased from Pressure Chemical Co. Ltd. NMR spectra were recorded on a Bruker ALX 300 spectrometer operating at 300 and 121.5 MHz for ^{1}H and ^{31}P, respectively. Chemical shifts (δ, ppm) were reported with reference to $SiMe_4$ (^{1}H) and H_3PO_4 (^{31}P). Infrared spectra (KBr) were recorded on a Perkin-Elmer 16 PC FT-IR spectrophotometer with use of pressed KBr pellets, and positive FAB mass spectra were recorded on a Finnigan TSQ 7000 spectrometer. The magnetic moment of the solid sample was measured by a Sherwood magnetic susceptibility balance at room temperature. Cyclic voltammetry was performed on a CHI 660 electrochemical analyzer. A standard three-electrode cell was used with a glassy carbon working electrode, a platinum counter electrode and an Ag/AgCl reference electrode under nitrogen atmosphere at 25 °C. Formal potentials (E^o) were measured in CH_2Cl_2 solutions with 0.1 M $[^nBu_4N]PF_6$ as supporting electrolyte and reported with reference to the ferrocenium-ferrocene couple ($Cp_2Fe^{+/0}$). In the −1.2 to +1.2 V region, a potential scan rate of 50 mV s^{-1} was used.

Table 1. Crystallographic data and experimental details for $[Ru^{III}(salen)(PPh_3)Cl] \cdot 2CH_2Cl_2$ (**1** $\cdot 2CH_2Cl_2$) and $[Ru^{II}$-(salen-NH)$(PPh_3)(CO)] \cdot CH_2Cl_2$ (**2** $\cdot CH_2Cl_2$).

Compound	**1** $\cdot 2CH_2Cl_2$	**2** $\cdot CH_2Cl_2$
Empirical formula	$C_{40}H_{33}N_2O_2Cl_5PRu$	$C_{40}H_{33}N_2O_3Cl_2PRu$
Formula weight	882.97	792.62
Crystal system	monoclinic	triclinic
Space group	$P2_1/n$	$P\bar{1}$
a, Å	13.1127(3)	9.2591(2)
b, Å	18.3256(4)	12.2474(3)
c, Å	16.9880(4)	17.3529(4)
α, deg	90	69.718(1)
β, deg	105.247(1)	79.291(1)
γ, deg	90	74.753(1)
V, Å^3	3938.50(16)	1771.07(7)
Z	4	2
D_{calc}, g cm^{-3}	1.49	1.49
Temperature K	296(2)	296(2)
$F(000)$, e	1788	808
$\mu(MoK_\alpha)$ mm^{-1}	0.8	0.7
Total / indep. refl. / R_{int}	38059 / 9060 / 0.022	32997 / 8111 / 0.026
Ref. parameters	460	441
$R1^a$ / $wR2^b$ [$I \geq 2\sigma(I)$]	0.0343 / 0.0854	0.0359 / 0.0925
$R1^a$ / $wR2^b$ (all data)	0.0466 / 0.0951	0.0421 / 0.0964
Goodness of fit (GoF)^c	1.03	1.04
$\Delta\rho_{fin}$ (max / min), e Å^{-3}	+0.64 / −0.61	+1.00 / −0.94

[a] $R1 = \Sigma||F_o| - |F_c||/\Sigma|F_o|$; [b] $wR2 = [\Sigma w(F_o^2 - F_c^2)^2 / \Sigma w(F_o^2)^2]^{1/2}$, $w = [\sigma^2(F_o^2) + (AP)^2 + BP]^{-1}$, where $P = (\mathrm{Max}(F_o^2, 0) + 2F_c^2)/3$; [c] $\mathrm{GoF} = [\Sigma w(F_o^2 - F_c^2)^2 / (n_{obs} - n_{param})]^{1/2}$.

Elemental analyses were carried out using a Perkin-Elmer 2400 CHN analyzer.

*Synthesis of $[Ru^{III}(salen)(PPh_3)Cl] \cdot 2CH_2Cl_2$ (**1** $\cdot 2CH_2Cl_2$)*

A mixture of H_2salen (85 mg, 0.75 mmol) and $[Ru(PPh_3)_3Cl_2]$ (671 mg, 0.70 mmol) in THF (40 mL) was refluxed with stirring for 4 h, during which time there was a color change from reddish brown to green. The solvent was evaporated *in vacuo*, and the residue was washed with diethyl ether and hexane. Recrystallization from CH_2Cl_2/hexane afforded green crystals of **1** $\cdot 2CH_2Cl_2$ within five days. Yield: 413 mg, 67 % (based on Ru). – IR (KBr disc, cm^{-1}): ν (C=N) 1591 (s). – MS (FAB): m/z = 711 $[M]^+$, 676 $[M\text{-}Cl]^+$, 449 $[M\text{-}PPh_3]^+$. – μ_{eff} = 1.94 μ_B. – Anal. for $C_{38}H_{27}N_2O_2ClPRu \cdot 2CH_2Cl_2$: calcd. C 54.41, H 3.77, N 3.17; found C 54.12, H 3.70, N 3.13.

*Synthesis of $[Ru^{II}(salen\text{-}NH)(PPh_3)(CO)] \cdot CH_2Cl_2$ (**2** $\cdot CH_2Cl_2$)*

A mixture of H_2salen (85 mg, 0.75 mmol) and $[RuHCl(CO)(PPh_3)_3]$ (666 mg, 0.70 mmol) in THF (40 mL) was refluxed with stirring for 6 h, during which time there was a color change from reddish grey to yellow. The solvent was evaporated *in vacuo*, and the residue was washed with diethyl ether and hexane. Recrystallization from CH_2Cl_2/hexane afforded yellow crystals of **2** $\cdot CH_2Cl_2$ within three days. Yield: 250 mg, 45 % (based on Ru). – ^{1}H NMR (300 MHz, $CDCl_3$): δ = 4.06 (d, J = 2.6 Hz, 2H, CH_2), 432 (br, 1H, N*H*), 531 (s, 2H, CH_2Cl_2), 7.11 – 7.93 (m, 27H, *Ph*), 882 (s, 1H, *H*C=N) ppm. – ^{31}P NMR (300 MHz, $CDCl_3$): δ = −3.46 ppm. – IR (KBr disc, cm^{-1}): ν(N-H) 3251 (w), ν(C≡O) 1947 (vs), ν(C=N) 1594 (s). – MS (FAB): m/z = 707 $[M]^+$, 679 $[M\text{-}CO]^+$, 445 $[M\text{-}PPh_3]^+$. – Anal. for $C_{39}H_{31}N_2O_3PRu \cdot (CH_2Cl_2)$: calcd. C 60.61, H 4.20, N 3.53; found C 60.23, H 4.11, N 3.49.

X-Ray crystallography

Crystallographic data and experimental details for $[Ru^{III}(salen)(PPh_3)Cl] \cdot 2CH_2Cl_2$ (**1** $\cdot 2CH_2Cl_2$) and $[Ru^{II}$-(salen-NH)$(PPh_3)(CO)] \cdot CH_2Cl_2$ (**2** $\cdot CH_2Cl_2$) are summarized in Table 1. Intensity data were collected on a Bruker SMART APEX 2000 CCD diffractometer using graphite-monochromatized MoK_α radiation (λ = 0.71073 Å) at 293(2) K. The collected frames were processed with the software SAINT [23]. The data were corrected for absorption using the program SADABS [24]. The structures were solved by Direct Methods and refined by full-matrix least-squares on F^2 using the SHELXTL software package [25, 26]. All non-hydrogen atoms were refined anisotropically. The positions of all hydrogen atoms were generated geometrically (C_{sp^3}-H = 0.97, C_{sp^2}-H = 0.93 and N-H = 0.86 Å), assigned isotropic displacement parameters, and allowed to ride on their respective parent carbon or nitrogen atoms before the final cycle of least-squares refinement.

CCDC 795838 and 795839 contain the supplementary crystallographic data for this paper. These data can be obtained free of charge from The Cambridge Crystallographic Data Centre *via* www.ccdc.cam.ac.uk/data_request/cif.

Results and Discussion

Treatment of $[Ru(PPh_3)_3Cl_2]$ with the Schiff base ligand H_2salen in THF at reflux afforded a neutral Ru^{III}-salen complex $[Ru^{III}(salen)(PPh_3)Cl]$ (**1**) as a green crystalline solid, while interaction of $[RuHCl$-$(CO)(PPh_3)_3]$ with H_2salen under similar conditions gave a neutral Ru^{II}-salen complex $[Ru^{II}(salen\text{-}NH)$-$(PPh_3)(CO)]$ (**2**) as a yellow crystalline solid, as illustrated in Scheme 1. The former was formed by displacement of one chloride and two PPh_3 ligands in the ruthenium starting material with ruthenium(II) being oxidized to ruthenium(III), and the deprotonated salen^{2-} group coordinated to the $[RuCl(PPh_3)]^{2+}$ species. The latter was similarly formed from the $[Ru$-$(CO)(PPh_3)]^{2+}$ species coordinating with the deproto-

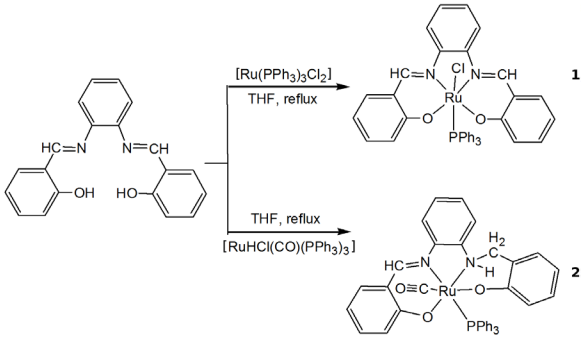

Scheme 1.

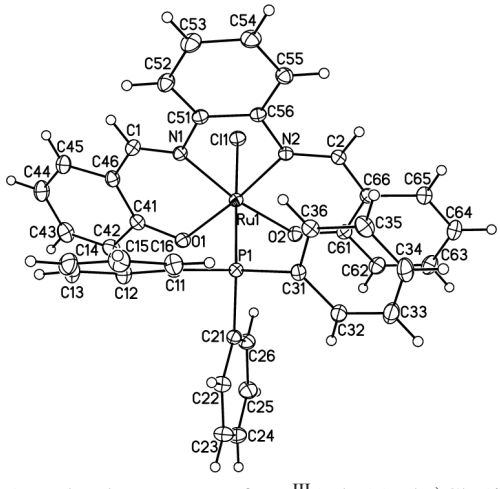

Fig. 1. Molecular structure of $[Ru^{III}(salen)(PPh_3)Cl]$ (**1**), in the crystal.

nated $(salen\text{-}NH)^{2-}$ group in which one of the imine bonds was nucleophilically attacked by hydride to result in the formation of a mixed imine-amine ligand.

The IR spectra of **1** and **2** clearly show strong bands at 1591 and 1594 cm^{-1}, respectively, which may be attributed to the ν(C=N) absorptions. The weak band at 3251 cm^{-1} in the IR spectrum of **2** may be tentatively assigned to the ν(NH) absorption. The C≡O stretching vibration mode was found at 1947 cm^{-1} in the IR spectrum of **2**. The effective magnetic moment μ_{eff} of 1.94 μ_B at r. t. is consistent with a ruthenium(III) formulation for **1** [18]. In the ^1H NMR spectrum of **2**, two ^1H signals at δ = 4.32 and 8.82 ppm are assigned to the protons of the amine NH and imine HC=N moieties, respectively. The $^{31}P\{^1H\}$ NMR spectrum of **2** shows a singlet at δ = −3.46 ppm, which is downfield from that of the free PPh_3 ligand. The positive ion FAB mass spectra of **1** and **2** display the peaks corresponding to the molecular ions $[M]^+$, $[M–Cl]^+$/$[M–CO]^+$ and $[M–PPh_3]^+$ with the characteristic isotopic distribution patterns.

Table 2. Selected bond lengths (Å) and angles (deg) for $\mathbf{1} \cdot 2CH_2Cl_2$.

Ru(1)–N(1)	1.9990(19)	Ru(1)–N(2)	2.0082(19)
Ru(1)–O(1)	2.0069(17)	Ru(1)–O(2)	2.0055(16)
Ru(1)–P(1)	2.3440(6)	Ru(1)–Cl(1)	2.4460(6)
N(1)–Ru(1)–N(2)	81.80(8)	O(1)–Ru(1)–O(2)	93.89(7)
N(1)–Ru(1)–O(1)	92.04(8)	N(1)–Ru(1)–O(2)	170.68(8)
O(1)–Ru(1)–N(2)	173.79(7)	O(2)–Ru(1)–N(2)	92.32(7)
O(1)–Ru(1)–P(1)	88.01(5)	O(2)–Ru(1)–P(1)	90.22(5)
N(1)–Ru(1)–P(1)	97.16(6)	N(2)–Ru(1)–P(1)	91.99(6)
N(1)–Ru(1)–Cl(1)	86.97(6)	N(2)–Ru(1)–Cl(1)	91.25(6)
O(1)–Ru(1)–Cl(1)	89.17(5)	O(2)–Ru(1)–Cl(1)	85.94(5)
P(1)–Ru(1)–Cl(1)	175.08(2)		

The crystal structures of $\mathbf{1} \cdot 2CH_2Cl_2$ and $\mathbf{2} \cdot CH_2Cl_2$ have been determined by X-ray crystallography. The molecular structure of $[Ru^{III}(salen)(PPh_3)Cl]$ (**1**) is shown in Fig. 1, and selected bond lengths and bond angles are given in Table 2. The geometry around the ruthenium atom is *pseudo*-octahedral with chloride and PPh_3 ligands in a mutually *trans* orientation, as indicated by the P(1)–Ru(1)–Cl(1) bond angle of 175.08(2)°. As expected, the N_2O_2 entity of the coordinated Schiff base lies in the equatorial plane. The Ru–O bond lengths of Ru(1)–O(1) = 2.0069(17) Å and Ru(1)–O(2) = 2.0055(16) Å, and the Ru–N bond lengths of Ru(1)–N(1) = 1.9990(19) Å and Ru(1)–N(2) = 2.0082(19) Å found for complex **1** are within the ranges found in other related Ru(III) complexes [14–19]. The Ru–Cl bond length of 2.4460(6) Å and the Ru–P bond length of 2.3440(6) Å are consistent with reported values [18, 19]. The bond angles of 170.68(8) and 173.79(7)° observed for N(1)–Ru(1)–O(2) and N(2)–Ru(1)–O(1), respectively, indicate a distortion from the ideal octahedral geometry.

Fig. 2 shows the molecular structure of $[Ru^{II}(salen\text{-}NH)(PPh_3)(CO)]$ (**2**), and selected bond lengths and bond angles are listed in Table 3. The molecule of **2** also adopts an approximately octahedral coordination around the ruthenium center as in **1**, but the positions *trans* to the carbonyl and PPh_3 groups are occupied by one hydroxyl and one imine moiety, respectively, indicated by the O(3)–Ru(1)–C(1) bond angle of 176.51(9)° and the N(2)–Ru(1)–P(1) bond angle of 178.42(6)°, with the carbonyl and the phosphine units *cis* to each other [C(1)–Ru(1)–P(1) = 89.00(8)°]. Obviously, the main change in the structure of the salen unit comes from the coexistence of aminic and

Table 3. Selected bond lengths (Å) and angles (deg) for $\mathbf{2} \cdot CH_2Cl_2$.

Ru(1)–N(1)	2.120(2)	Ru(1)–N(2)	2.068(2)
Ru(1)–C(1)	1.833(3)	Ru(1)–O(2)	2.0552(17)
Ru(1)–O(3)	2.0892(18)	Ru(1)–P(1)	2.3447(6)
C(1)–O(1)	1.151(3)		
N(1)–Ru(1)–N(2)	80.17(8)	O(2)–Ru(1)–N(1)	169.26(7)
O(3)–Ru(1)–N(1)	88.72(8)	O(2)–Ru(1)–N(2)	92.39(7)
O(3)–Ru(1)–N(2)	85.49(7)	C(1)–Ru(1)–N(1)	90.58(10)
C(1)–Ru(1)–N(2)	91.02(9)	C(1)–Ru(1)–O(2)	97.33(9)
C(1)–Ru(1)–O(3)	176.51(9)	O(2)–Ru(1)–O(3)	82.94(7)
C(1)–Ru(1)–P(1)	89.00(8)	O(2)–Ru(1)–P(1)	89.17(5)
N(2)–Ru(1)–P(1)	178.42(6)	O(3)–Ru(1)–P(1)	94.49(5)
N(1)–Ru(1)–P(1)	98.25(6)		

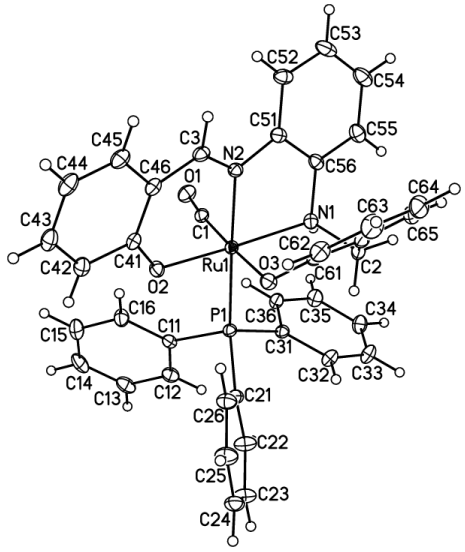

Fig. 2. Molecular structure of $[Ru^{II}(salen\text{-}NH)(PPh_3)(CO)]$ (**2**), in the crystal.

iminic bonds. The torsion angle for the iminic bond C(51)–N(2)–C(3)–C(46) is 177.7°, while that for the amine bond C(56)–N(1)–C(2)–C(66) is 58.1°. The mixed imine-amine ligand is twisted from the regular butterfly conformation of the salen ligand to a V-shaped conformation. The only similar example for the salophen ligand is a dimeric aluminum-salophen complex [27]. The hydrogen atoms on the newly formed sp^3 atoms [N(1) and C(2)] have enough space in **2** and do not affect the relative orientation of phenyl groups. The sterical crowding around the new sp^3 atoms is relaxed by the V shape of the ligand so that abnormal torsion angles around N(1) and C(2) are avoided. The Ru–P bond length of 2.3447(6) Å is comparable to that in other ruthenium phosphine complexes such as $[Ru(2\text{-}Br\text{-}salen)_2(PPh_3)_2]$ [av. 2.403(2) Å] [14] and **1** [2.3440(6) Å]. The Ru–C bond length (1.833(3) Å) in **2** is in good agreement with that in $[Ru(3,5\text{-}t\text{-}Bu_2salen)(CO)_2] \cdot 3MeOH$ [3,5-*t*-Bu_2salen = *NN*′(di-3,5-di-*t*-butyl-2-oxybenzylidene)-cyclohexane-1,2-diamine] (av. 1.874(2) Å), [Ru(3-*t*-Bu-salen)$(CO)_2$] [3-*t*-Bu-salen = *NN*′(di-3-*t*-butyl-2-oxybenzylidene)cyclohexane-1,2-diamine] (av. 1.881(3) Å) [28], and [Ru(2-Br-salen)(CO)(MeIm)] (MeIm = *N*-methylimidazole) (1.846(13) Å) [14], but slightly shorter than that in *cis*-,*cis*-$[Ru\{\eta^2\text{-}N(O)C_{10}H_6\}]_2(CO)(PPh_3)]$ (1.919(4) Å) [29].

The cyclic voltammogram of **1** shows three reversible oxidation couples at $E_{1/2}$ = 0.82, 0.58 and −0.87 V, which are assigned to the metal-centered Ru^{III}-Ru^{II} couple, the ligand-centered oxidation, and the metal-centered oxidation of Ru^{IV}-Ru^{III}, respectively. The Ru^{III}-Ru^{II} potential for complex **2** ($E_{1/2}$ = 0.94 V) is considerably larger than that for complex **1** ($E_{1/2}$ = 0.82 V), indicative of the carbonyl stabilization of the complex. It is also noted that the cyclic voltammogram of **1** reveals two reversible couples at 0.94 and 0.61 V assigned to the Ru^{III}-Ru^{II} couple and ligand-centered oxidation, respectively. Similar to complex [Ru(salen)(NO)Cl] [13], the irreversible wave at −0.91 V in complex **1** is assigned to the metal-centered reduction of ruthenium(II).

In summary, the ruthenium(III)-salen complex $[Ru^{III}(salen)(PPh_3)Cl]$ (**1**) and the ruthenium(II)-salen complex $[Ru^{II}(salen\text{-}NH)(PPh_3)(CO)]$ (**2**) with triphenylphosphine ligands were synthesized and structurally characterized along with spectroscopic and electrochemical analyses. Formation of **1** involved the oxidation of ruthenium(II) to ruthenium(III), and formation of **2** involved the generation of a mixed imine-amine ligand salen-NH, which is due to one of the imine bonds being nucleophilically attacked by hydride. It is interesting to note that the mixed imine-amine ligand is twisted from the regular butterfly conformation of the salen ligand to a V-shaped conformation, which results in the carbonyl and the phosphine ligands being *cis* to each other so as to avoid the sterical crowding around the octahedral ruthenium center in **2**. The catalytic properties of these rutheniumsalen complexes will be further investigated in our laboratory.

Acknowledgement

This project was supported by the Natural Science Foundation of China (20771003) and the Program for New Century Excellent Talents in University of China (NCET-06-0556).

[1] R. J. Crutchky, *Adv. Inorg. Chem.* **1994**, *41*, 273.
[2] S. Nag, P. Gupta, R. J. Butcher, S. Bhattacharya, *Inorg. Chem.* **2004**, *43*, 4814.
[3] R. Acharyya, S.-M. Peng, G. H. Lee, S. Bhattacharya, *Inorg. Chem* **2003**, *42*, 7378.
[4] T. Koiwa, Y. Masuda, J. Shono, Y. Kawmoto, Y. Hashino, T. Hashimoto, K. Natarajan, K. Shimizu, *Inorg. Chem*. **2004**, *43*, 6215.
[5] O. Novakova, J. Kasparkova, O. Vrana, P. M. Vanvliet, J. Reedijik, V. Brabec, *Biochemistry* **1995**, *34*, 12369.
[6] G. D. Frey, Z. R. Bell, J. C. Jeffery, M. D. Ward, *Polyhedron* **2001**, *20*, 3231.
[7] P. A. Vigato, S. Tamburini, *Coord. Chem. Rev*. **2004**, *248*, 1717.
[8] E. N. Jacobson, M. H. Wu in *Comprehensive Asymmetric Catalysis II*, (Eds.: E. N. Jacobson, A. Pfaltz, H. Yamamoto) Springer Berlin, **1999**, pp. 649 – 667.
[9] J. A. Miller, B. A. Gross, M. A. Zhuravel, W. Jin, S. T. Nguyen, *Angew. Chem.* **2005**, *117*, 3953; *Angew. Chem. Int. Ed.* **2005**, *44*, 3885.
[10] W. L. Man, H. K. Kwong, W. W. Y. Lam, J. Xiang, T. W. Wong, W. H. Lam, W. T. Wong, S. M. Peng, T. C. Lau, *Inorg. Chem.* **2008**, *47*, 5936.
[11] C. M. Che, C. K. Poon, *Pure Appl. Chem*. **1998**, *60*, 1201.
[12] C. M. Che, W. T. Tang, W. T. Wong, T. F. Lai, *J. Am. Chem. Soc.* **1989**, *111*, 9048.
[13] W. H. Leung, E. Y. Y. Chan, E. K. F. Chow, I. D. Williams, S. M. Peng, *J. Chem. Soc., Dalton Trans.* **1996**, 1229.
[14] G. Y. Li, J. Zhang, P. W. H. Chan, Z. J. Xu, N. Zhu, C. M. Che, *Organometallics* **2006**, *25*, 1676.
[15] X. G. Zhou, J. S. Huang, P. H. Ko, K. K. Cheung, C. M. Che, *J. Chem. Soc., Dalton Trans.* **1999**, 3303.
[16] J. Bordini, D. L. Hughes, J. D. Da Motta Neto, C. J. da Cunha, *Inorg. Chem* **2002**, *41*, 5410.
[17] W. L. Man, T. M. Tang, T. W. Wong, T. C. Lau, S. M. Peng, W. T. Wong, *J. Am. Chem. Soc.* **2004**, *126*, 478.
[18] P. M. Chan, W. Y. Yu, C. M. Che, K. K. Cheung, *J. Chem. Soc., Dalton Trans*. **1998**, 3183.
[19] R. Prabhakaran, R. Huang, K. Natarajan, *Inorg. Chim. Acta* **2006**, *359*, 3359.
[20] T. A. Stephenson, G. Wilkinson, *J. Inorg. Nucl. Chem* **1966**, *28*, 945.
[21] U. Kölle, J. Kossakowski, *Inorg. Synth* **1992**, *29*, 225
[22] O. Meth-Cohn, B. Tarnowski, *Synthesis* **1978**, 56.
[23] SMART and SAINT+ for Windows NT (version 6.02a), Bruker Analytical X-ray Instruments Inc., Madison, Wisconsin (USA) **1998**.
[24] G. M. Sheldrick, SADABS, Program for Empirical Absorption Correction of Area Detector Data, University of Göttingen, Göttingen (Germany) **1996**.
[25] G. M. Sheldrick, SHELXTL (version 5.1) Software Reference Manual, Bruker AXS Inc., Madison, Wisconsin (USA) **1997**.
[26] G. M. Sheldrick, *Acta Crystallogr.* **1990**, *A46*, 467; *ibid.* **2008**, *A64*, 112.
[27] M. Cametti, A. D. Cort, M. Colapietro, G. Portalone, L. Russo, K. Rissanen, *Inorg. Chem.* **2007**, *46*, 9057.
[28] Z. J. Xu, R. Fang, C. Zhao, J. S. Huang, G. Y. Li, N. Zhu, C. M. Che, *J. Am. Chem. Soc.* **2009**, *131*, 4405.
[29] X. X. Liu, W. T. Wong, *Polyhedron* **2000**, *19*, 7.